

Bio-Composites for Additive Manufacturing: Study of the Mechanical Properties

Francisco Comino^{1,a}, José A. Martínez-Sánchez^{1,b}, Marco Zaza^{2,c},
Sabina Campanelli^{3,d}, Roberto Spina^{3,4,5,e*}

¹Departamento de Mecánica, Universidad de Córdoba, Spain

²Crea3D, Bari, Italy

³Dip. di Meccanica, Matematica e Management, Politecnico di Bari, Italy

⁴Istituto Nazionale di Fisica Nucleare (INFN) - Sezione di Bari, Italy

⁵Consiglio Nazionale delle Ricerche - Istituto di Fotonica e Nanotecnologie (CNR-IFN), Italy

^afrancisco.comino@uco.es, ^bz12masaj@uco.es, ^cmarco.zaza@crea3d.com,

^dsabinaluisa.campanelli@poliba.it, ^{e*}roberto.spina@poliba.it

*corresponding author

Keywords: composite, natural fibers, mechanical properties, material extrusion.

Abstract. The objective of the present research was to identify the mechanical properties of 3D-printed biocomposite parts and their variation with different natural fillers (olive wood and almond shell). The materials were produced by filament extrusion with 5% fiber content in the polylactic acid matrix, and the samples were fabricated using the Material Extrusion Additive Manufacturing process. 3D printed specimens underwent tensile and flexural tests to assess their mechanical properties. The results showed reductions of 5-18% in the tensile modulus and 10- 38% in the tensile strength for PLA based on olive wood and almond shell, respectively. The same trend was observed for the flexural properties, with a 2-3% reduction in flexural modulus and a 3-5% reduction in flexural strength.

Introduction

Progress in bio-composites has gained significant importance due to growing concerns about environmental issues associated with the use of petroleum-derived synthetic polymers. The use of eco-friendly reinforcing materials and their fabrication are crucial topics because they offer several advantages, including low cost, abundance, and minimal environmental impact. Matrices are natural/bio-derived polymers, whereas the reinforcing agents are also either bio-or synthetic fibers. These bio-composites are not only biodegradable but also bio-compatible, especially when both components are bio-based [1]. The recovery of agricultural waste (agro-waste), typically managed through incineration, composting, or landfilling, offers new opportunities to reuse a wide range of materials, from crop residues such as straw and stalks to fruit and vegetable peels and nut shells. There is a need to develop innovative methods for the utilization of agro-waste [2]. By embracing circular economy principles, industries can substantially reduce waste and greenhouse gas emissions, enhance product durability, and enhance resource efficiency through recycling and reuse initiatives.

In this context, polylactic acid (PLA), a thermoplastic polymer derived from renewable resources and reinforced with natural fibers, is a promising candidate for use in biocomposites. PLA is among the most promising biopolymers because its monomers can be produced from non-toxic, renewable feedstocks and are naturally occurring organic acids [3]. There is a frequent need to reinforce PLA to achieve properties suitable for consumer, packaging, and biomedical applications [4]. However, early formulations of bio-composites exhibited inferior mechanical strength, thermal stability, and barrier properties relative to conventional composites, thereby limiting their widespread adoption [5]. Natural fibers are an efficient option for enhancing aesthetic properties while maintaining the sustainability of the final part. Among natural fiber sources, olive wood and almond shell stand out

for their availability in Mediterranean regions and favorable physical properties, making them attractive for incorporation into composite materials.

This study investigates bio-composites comprising olive wood (OW) and almond shell (AS) fibers produced via filament extrusion, with 5% fiber content in the PLA matrix, and 3D samples printed using the Material Extrusion (MEX) Additive Manufacturing process. Additively manufactured specimens undergo several tests to assess their mechanical properties. This study compares the mechanical properties of 3D specimens fabricated from these bio-composites, evaluates their sustainability in industrial applications, and assesses their potential in various engineering applications.

Materials and Methods

Poly(lactic acid) (PLA) is a bio-based, biodegradable aliphatic polyester. As a semicrystalline thermoplastic, PLA exhibits excellent mechanical and physical properties, attracting significant interest in several industries [6]. Net PLA was supplied in pellets, while olive wood (OW) and almond shell (AS) fiber particles were obtained by collecting and recycling agricultural waste. Polylactic acid (PLA) Ingeo 4043D (NatureWorks, USA) and Luminy LX175 (TotalEnergies Corbion, The Netherlands) were selected as the polymer matrices, with the primary data reported in Table 1. Both PLAs exhibited similar thermal and mechanical properties, with a melt flow index of 6 g/min and a natural color [7, 8].

Table 1. Material range data.

Physical property	Value	Physical property	Value
Density ρ	1.24 [g/cm ³]	Tensile strength σ_R	45-60 [MPa]
Glass transition temperature T_g	55-60 [°C]	Young's modulus E	3.5-3.6 [GPa]
Melt temperature T_m	145-160 [°C]	Strain at break ε_{tb}	5-6 [%]

The AS and OW fiber particles were milled and sieved to a size below 200 μm to ensure stable filament extrusion and minimize clogging. The incorporation of natural particles enabled the creation of lighter components, as their lower density than PLA results in rougher surfaces and increased porosity [9]. Before compounding, PLA pellets and fibers were oven-dried at 60 °C for 8 h to reduce residual moisture, limit hydrolytic degradation, and bubble formation during melt processing. The 1.75 mm filaments (tolerance ± 0.03 mm) were produced using a single-screw extruder equipped with temperature control and an in-line laser diameter gauge, incorporating 5% by weight of the selected filler.

The specimens were fabricated using the MEX E2 printer (Raise 3D Technologies Inc., USA), which employed two independent dual-extruder heads (IDEX) that moved along the X -axis. The maximum build volume was 330×240×240 mm³ for a single extrusion print. All dog-bone samples were designed in accordance with ISO 527-2:2012 [10], with envelope dimensions of 150×20×4 mm³. The 3-point bending samples were designed in accordance with ISO 178:2019 [11], and had dimensions of 80×10×4 mm³. All specimens were printed with a nozzle diameter of 800 μm , a layer height of 350 μm , 100% infill, and one layer for the top and bottom, and one layer for each side wall. The number of walls and layers was selected to ensure sufficient resistance to external loads along the central axis during the tensile test without unduly affecting the internal pattern. The internal linear infill pattern was $\pm 45^\circ$ and $0^\circ/90^\circ$ for tensile and flexural specimens, respectively. The main MEX parameters were the printing speed v (60 mm/s), the nozzle temperature T_N (230°C), and the build plate temperature T_B (55°C). All specimens were printed flat on the build platform (XY plane) on the same platen, once per time, to avoid mutual influence during cooling. The deposition paths generated using the proprietary slicer software, ideaMaker, are presented in Figure 1.

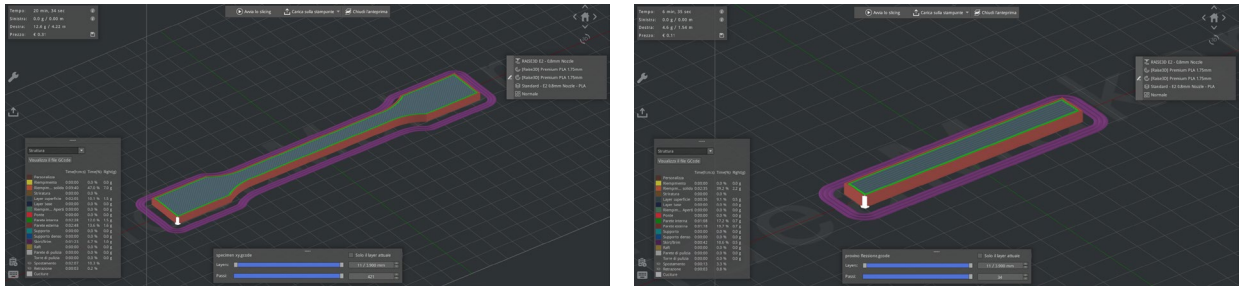


Fig. 1. Specimen slices with ideaMaker (Raise 3D Technologies Inc.).

The mechanical properties of the MEX samples were assessed using an uniaxial testing machine, which enabled characterization of their elastic and plastic behavior under monotonic loading. Mechanical tests on dog-bone and flexural specimens were conducted on an ETM type A universal single-column testing machine (Wance Testing Machine Co., Ltd., Shenzhen, China) with a 5 kN load cell (accuracy of $\pm 0.5\%$) and a crosshead travel (without grip) of 1,000 mm (accuracy of $\pm 0.5\%$). According to ISO 527-1:2019 [12] and ISO 178:2019 [11], measurements were performed in a temperature-controlled environment at a transverse speed of 5 mm/min, with a maximum deviation of ± 0.5 °C from the ambient temperature. Five repetitions per set were carried out, and the results were averaged.

Results

The produced MEX specimens are shown in Figure 2 for net PLA and for both PLA/fiber combinations. PLA/AS and PLA/OW indicate the PLA with almond shell (AS) and olive wood (OW), respectively. Evident color variations were observed among the materials: the net PLA retained its natural color, whereas the fibers imparted their own color to the original PLA matrix in PLA/AS and PLA/OW. The Red-Green-Blue (RGB) color model was used, in which each channel parameter specified the color's intensity, with values ranging from 0 to 255. At the same time, the RGB value was converted to a hexadecimal code. The average RGB values measured were #ada99e (173, 169, 158) for natural PLA, #7a6450 (122, 100, 80) for PLA/AS, and #5f4c3f (95, 76, 63) for PLA/OW. Figure 3 presents histograms of the material, split by each RGB component. The addition of the fiber made the material darker in all RGB components, with PLA/OW consequently the darkest. Additionally, the shape of each signal shifted from symmetrical (PLA) to skewed (PLA/AS) to bimodal (PLA/OW).

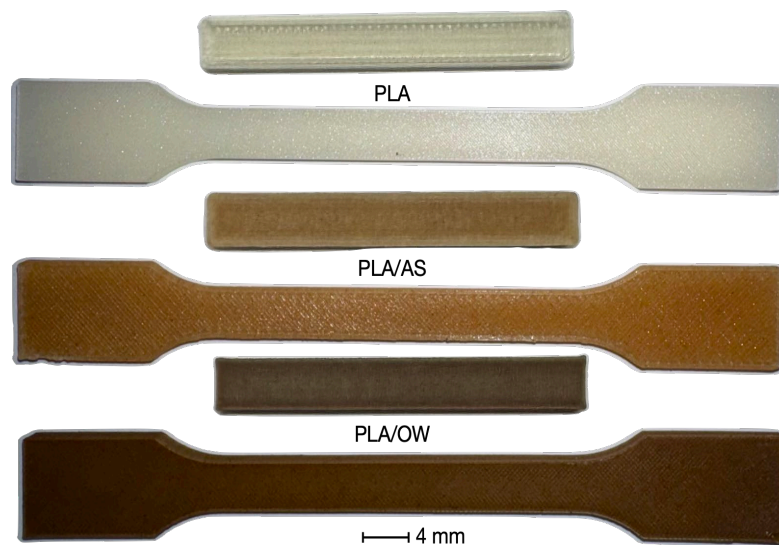


Fig. 2. MEX specimens.

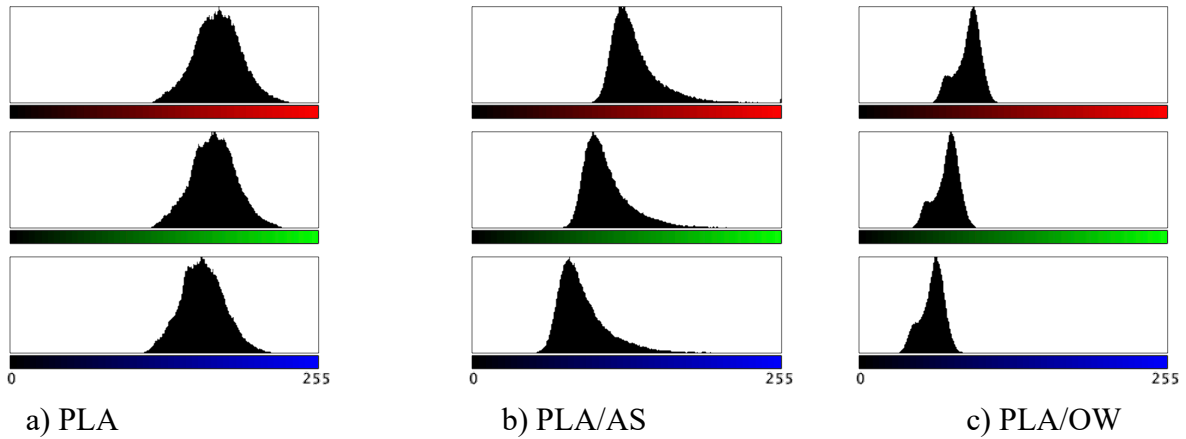


Fig. 3. RGB values.

The mechanical tests were performed on all specimens. The investigation started with the tensile test. The initial cross-section of each MEX specimen was measured before testing using a digital micrometer. The maximum strain ε was set to 4% for each test, denoted as $\varepsilon_{4\%}$, based on previous studies in which the maximum stress was reached at this value [13]. All specimens fractured in a brittle manner, with a very limited plateau observed above the yield point and a low-stress drop. Moreover, the elongation and tensile toughness values (as indicated by the area under the stress-strain curve) were higher than those specified in the material data sheet. Table 2 lists the tensile properties of the printed specimens, including Young's modulus E , ultimate tensile strength σ_R , and strain at break ε_{th} . A portion of the stress-strain curves between 5 and 20 MPa was used to calculate the E modulus. The low value of 5 MPa was needed to achieve load stabilization during testing.

Table 2. Tensile material results.

Material	E [GPa]	σ_R [MPa]	ε_{th} [%]
<i>PLA</i>	2.39 ± 0.06	50.47 ± 0.62	3.77 ± 0.22
<i>PLA/AS</i>	1.97 ± 0.13	31.58 ± 1.96	1.95 ± 0.14
<i>PLA/OW</i>	2.28 ± 0.06	45.23 ± 1.07	3.13 ± 0.04

The performance of MEX specimens made with the PLA and fibers was lower than that of those with net PLA, likely due to reduced interfacial adhesion, which affected the composite's mechanical properties, as identified in a previous work [14]. The presence of voids was identified, resulting from incomplete bonding or fiber particle agglomeration during compounding. Figure 4 reports normalized values, with the PLA results used as the reference at 100 to highlight the reduction, using the formula $P_{norm} = (1 - P/P_{PLA}) \times 100$, where P was the generic property (E , σ_R , and ε_{th}) and P_{PLA} the same property for the net PLA.

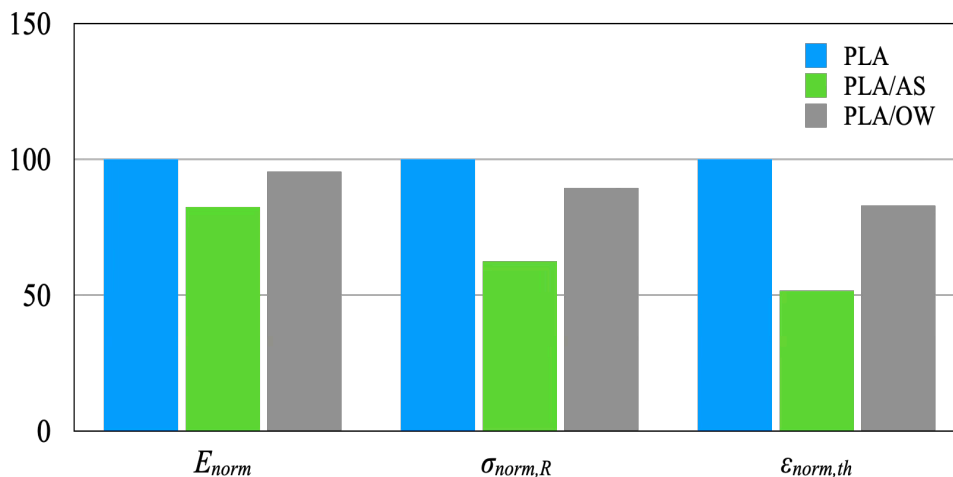


Fig. 4. Tensile results.

The reductions in E modulus were 17.6% and 4.6% for PLA/AS and PLA/OW, respectively. These outcomes suggested that the interfacial adhesion of the AS fibers to the PLA matrix was lower than that of the OW fibers. The same trend was observed for the tensile strength σ_R , with reductions of 37.4% and 10.4% with respect to the net PLA. The decrease in the strain at break ε_{th} with respect to the net PLA was more pronounced, with values of 48.3% and 17.0% for PLA/AS and PLA/OW, respectively. Based on the above results, adding OW fibers to the PLA matrix was more effective than adding AS fibers. The results also revealed that the variation in the response variables was less than 10% for PLA and PLA/OW, indicating that the test was repeatable relative to the median. The PLA/AS deviation was 17%, suggesting, once again, that low adhesion may be the primary cause of the poor performance.

The mechanical analysis was extended to flexural testing to determine essential material properties, including the flexural modulus E_f , the maximum flexural stress σ_{fM} , and the flexural strain at fracture ε_{fb} . The average results of the flexural tests conducted on MEX specimens are presented in tabular form (Table 3) for all materials, using a span distance of 64 mm.

Table 3. Flexural results.

Material	E_f [GPa]	σ_{fM} [MPa]	ε_{fb} [%]
PLA	1.86 ± 0.02	56.57 ± 0.77	6.08 ± 0.11
PLA/AS	1.81 ± 0.05	54.17 ± 0.61	3.60 ± 0.17
PLA/OW	1.80 ± 0.01	55.17 ± 0.56	4.45 ± 0.10

The decrease in the E_f modulus were 2.7% and 3.2% for PLA/AS and PLA/OW, respectively, and in the flexural strength, σ_{fM} were 4.2% and 2.5% with respect to the net PLA. These reductions below 5% indicated the good performance of the MEX specimens when AS and OW fibers were added to the net PLA. However, the decreases in flexural strain were 59.2% and 73.2% for PLA/AS and PLA/OW, respectively, highlighting a deterioration in the flexibility of the MEX specimens with fibers. The normalized flexural results were presented in graphical form in Figure 5. Based on the results of the tensile test, the addition of the OW fibers to the PLA matrix was better than the addition of the AS fibers. The mechanical test results also revealed that the variation in response variables was very low for PLA and PLA/OW, indicating that the test was repeatable relative to the median value. The most significant variation was observed for PLA/AS, suggesting, once again, that low adhesion between AS fibers and the matrix was the primary factor.

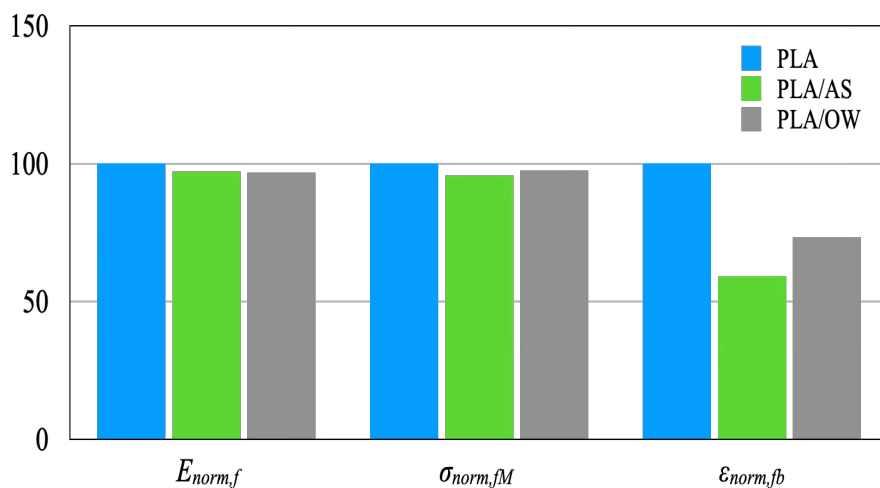


Fig. 5. Flexural results.

Conclusion

This study evaluated the mechanical response of MEX 3D-printed PLA biocomposites containing 5 wt: % olive wood (OW) and almond shell (AS) particles. The results confirm that both fillers can be successfully processed into printable filaments and manufactured into stable parts, while also providing clear visual differentiation of the materials, as reflected in the measured RGB values. Mechanically, the incorporation of natural fillers enabled the composites to retain flexural performance comparable to that of neat PLA, with only minor (<5%) changes in flexural modulus and strength, supporting their potential use in applications primarily subjected to bending loads. In tension, a moderate reduction in stiffness and strength was observed, particularly for AS, indicating that the filler type plays an important role even at low loading levels. Additionally, the lower strain at break suggests a shift towards less ductile behavior, which should be considered for components that require large deformations. Overall, PLA provided the most balanced combination of mechanical retention and bio-based aesthetic enhancement, reinforcing the interest of these sustainable biocomposites for functional 3D-printed parts with moderate mechanical requirements.

Acknowledgment

The Project was funded under the following programs:

- Department of Excellence - Law number 232/2016 (Grant No. CUP - D93C23000100001).
- The National Recovery and Resilience Plan (NRRP), Mission 4 Component 2 Investment 1.3 - Call for tender No. 341 of 15/03/2022 of the Italian Ministry of University and Research (MUR), funded by the European Union - NextGenerationEU.
- Space It Up project funded by the Italian Space Agency, ASI, and the Italian Ministry of University and Research (MUR) under contract n. 2024-5-E.0 (Grant No. CUP-I53D24000060005).
- European Innovation Association (AEI) on agricultural productivity and sustainability for the creation and operation of operational groups and the Ministry of Agriculture, Livestock, Fisheries, and Sustainable Development of the Junta de Andalucía through the research project AGROSEC, reference GOPO-JA-23.

References

- [1] N Karak. *Advances in Biocomposites and their Applications* (2024) 1-39. doi:10.1016/B978-0-443-19074-2.00001-0.
- [2] GO Edah, JO Atiba, OSI Fayomi. *Advancements in fibre-reinforced polymers: Properties, applications*. *Next Mat.* 8 (2025) 100743. doi:10.1016/j.nxmte.2025.100743.
- [3] S Farah, DG Anderson, R Langer. *Physical and mechanical properties of PLA, and their functions in widespread applications - A comprehensive review*. *Adv. Drug Delivery Rev.* 107 (2016) 367-392. doi:10.1016/j.addr.2016.06.012.
- [4] R Spina. *Performance analysis of colored PLA products with a Fused Filament Fabrication Process*, *Polymers.* 11 (2019) 1984. doi:10.3390/polym11121984.
- [5] DK Chandra, A Kumar, C Mahapatra. *Ecofriendly bioplastics from biowaste: Antimicrobial and functional enhancements for sustainable packaging*. *European Polymer Journal* 221 (2024) 113557. doi:10.1016/j.eurpolymj.2024.113557.
- [6] C Hu, Y Zhang, X Pang, X Chen. *Poly(LacticAcid): Recent Stereochemical Advances and New Materials Engineering*. *Adv. Mater.* 37 (2024) 2412185. doi:10.1002/adma.202412185.
- [7] Ingeo Biopolymer 4043D Technical Data Sheet.
- [8] TotalEnergies Corbion Luminy LX175 Data Sheet.

-
- [9] JA Martínez-Sánchez et al. Design, development, and performance evaluation of a 3D-printed desiccant wheel using poly-lactic acid and wood filaments for sustainable HVAC systems. *Build. Environ.* 276 (2025) 112889. doi:10.1016/j.buildenv.2025.112889.
- [10] Plastics - Determination of tensile properties - Part 2: Test conditions for moulding and extrusion plastics (ISO 527-2:2012).
- [11] Plastics - Determination of flexural properties (ISO 178:2019).
- [12] Plastics - Determination of tensile properties - Part 1: General principles (ISO 527-1:2019).
- [13] R Spina. Surface appearance of poly lactic acid due to variations in material extrusion processing parameters. *Sci. Rep.* 15 (2025) 29788. doi:10.1038/s41598-025-14484-0.
- [14] F Comino et al. Thermo-mechanical properties of polylactic acid/olive wood composite for additive manufacturing. *Mater. Res. Proc.* 54 (2025) 2344-2351. doi:10.21741/9781644903599-253.